ANODIC ZIRCONIUM DIOXIDE-BASED NANOTUBES FOR PHOTOREDUCTION OF HEXAVALENT CHROMIUM (Cr(VI))

NURULHUDA BINTI BASHIROM

UNIVERSITI SAINS MALAYSIA

2019

ANODIC ZIRCONIUM DIOXIDE-BASED NANOTUBES FOR PHOTOREDUCTION OF HEXAVALENT CHROMIUM (Cr(VI))

by

NURULHUDA BINTI BASHIROM

Thesis submitted in fulfilment of the
requirements for the degree of
Doctor of Philosophy

March 2019

ACKNOWLEDGEMENT

Alhamdulillah, praise to Allah SWT the Almighty and peace and blessings be upon the Prophet Muhammad SAW because with the courage and patient, I was able to complete my Ph.D. study. I take this opportunity to express my profound gratitude to everyone that involved and supported me throughout this journey.

A special thanks goes to my supervisor, Assoc. Prof. Dr. Zainovia Lockman for the patient guidance, encouragement and advice provided during this study. I would also like to thank Mr. Rashid, Mr. Azam, Mr. Khairi, and all other staff in the School of Materials and Mineral Resources Engineering, Universiti Sains Malaysia (USM) for their kindness and cooperation towards the completion of this study. I am also greatly indebted to my colleagues Azhar, Monna, Nyein Nyein, and Izza for their advice and guidance. Their willingness to share their knowledge and their help in this research.

The Heavy Metal Mitigation project was supported by USM Research University Grant for Toyohashi University of Technology, Japan-USM collaboration (1001/PBAHAN/870048). Crystallization of anodic oxide work was supported by the Fundamental Research Grant Scheme, Ministry of Education Malaysia (1001/PBAHAN/6071363).

Finally, I also thank my family; my beloved husband Mr. Muhammad Najib Bin Saedi and my lovely son Muhammad Ikram Bin Muhammad Najib for their sacrifice and understanding. To my parents Mr. Bashirom Bin Hassan and Mrs. Hasnah Binti Shaari for continuous support and encouragement throughout my years of study. Thanks also to my employer Universiti Malaysia Perlis (UniMAP) and

Ministry of Education Malaysia for giving me the golden opportunity to pursue my study here and for supporting my Ph.D. scholarship.

TABLE OF CONTENTS

Page

CHAPTER ONE : INTRODUCTION

CHAPTER TWO : LITERATURE REVIEW

CHAPTER THREE : MATERIALS AND METHODS

CHAPTER FOUR : RESULTS AND DISCUSSION

CHAPTER FIVE : CONCLUSION AND RECOMMENDATIONS

APPENDICES

LIST OF TABLES

LIST OF FIGURES

Page

LIST OF ABBREVIATIONS

BET	Brunauer-Emmett-Teller
CNTs	Carbon nanotubes
Cr(VI)	Hexavalent chromium
Cr(III)	Trivalent chromium
CRL	Carbon-rich layer
CB	Conduction band
c-ZrO_2	Cubic-ZrO_2
DFT	Density functional theory
DOS	Density of states
DPC	1,5-Diphenylcarbazide
DI	Deionized
DMF	Dimethylformamide
EC	Electrocoagulation
EF	Electroflotation
ED	Electrodeposition
EG	Ethylene glycol
EDTA	Ethylenediaminetetraacetic acid
EPR	Electron paramagnetic resonance
FSZNTs	Freestanding ZrO_2 nanotubes
FNTs	Iron oxide nanotubes
FA	Formamide
FESEM	Field emission scanning electron microscope
FTO	Fluorine doped tin oxide

FTIR	Fourier-transform infrared
FRL	Fluoride-rich layer
F	α-Fe_2O_3
FZ	Fe_2O_3-ZrO_2
FZC	Fe_2O_3-ZrO_2-surfactant
HRTEM	High resolution transmission electron microscope
HOMO	Highest occupied molecular orbital
1-D	One-dimensional
ISO	International Organization for Standardization
IR	Infrared
LUMO	Lowest unoccupied molecular orbital
MO	Methyl orange
m-ZrO_2	Monoclinic-ZrO_2
NHE	Normal hydrogen electrode
NTs	Nanotubes
NPs	Nanoparticles
NCs	Nanochannels
N/A	Not available
Ortho-$ZrTiO_4$	Orthohombic-$ZrTiO_4$
PL	Photoluminescence
PZC	Point zero charge
PRED	Pulse reverse electrodeposition
RBA	Rapid breakdown anodization
TG-DTA	Thermogravimetry-differential thermal analysis
TNTs	TiO_2 nanotubes

TEM	Transmission electron microscope
t-ZrO_2	Tetragonal-ZrO_2
UV	Ultraviolet
US-EPA	US Environmental Protection Agency
vs.	Versus
VB	Valence band
XPS	X-ray photoemission spectroscopy
XRD	X-ray diffraction
ZNTs	ZrO_2 nanotubes
ZTNTs	ZrO_2-TiO_2 nanotubes
ZFNTs	ZrO_2-α-Fe_2O_3 nanotubes

LIST OF SYMBOLS

A	Ampere
α	Absorption coefficient
E_g	Band gap
cm	Centimeter
cm^3	Cubic centimeter
E_{CB}	Conduction band edge potential
I	Current
i	Current density
j_{cr}	Critical current density
U	Constant applied voltage
2θ	Diffraction angle
°C	Degree celsius
D	Diameter
D	Diffusion coefficient
F	Driving force
e^-	Electron
eV	Electrovolt
E	Electric field strength
ΔU_{appl}	Externally applied voltage
fs	Femtoseconds
g	Gram
h	Hour
D_i	Inner diameter
L	Length
<	Less than
>	More than
mg	Milligram
µm	Micrometer
mm	Millimeter

mL	Milliliter
M	Molarity
min	Minute
nm	Nanometer
ns	Nanosecond
d	Oxide thickness
D_o	Outer diameter
$h\nu$	Photon energy
%	Percentage
ps	Picosecond
r	Radius of spherical particle
R	Resistivity
s	Second
ts	Terasecond
T	Temperature
E_{VB}	Valence band edge potential
V	Volt
η	Viscosity
wt.%	Weight percentage
λ	Wavelength
W_t	Wall thickness

TIUBNANO BERASASKAN ANODIK ZIRKONIUM DIOKSIDA UNTUK FOTOPENURUNAN KROMIUM ENAM (Cr(VI)

ABSTRAK

Pencemaran air oleh ion-ion logam berat seperti kromium enam, Cr(VI) menjadi salah satu kebimbangan utama global. Pendedahan kepada Cr(VI) boleh menyebabkan masalah kesihatan yang teruk kerana ia adalah bahan karsinogen. Penyingkiran Cr(VI) daripada punca air kumbahan perlu dilakukan. Salah satu kaedah untuk menyingkirkan Cr(VI) daripada air kumbahan industri ialah melalui penurunan Cr(VI) kepada Cr(III) yang kurang berbahaya di atas foto-mangkin yang sesuai. Tiubnano berasaskan ZrO_2 difabrikasikan untuk fotopenurunan Cr(VI): tiubnano ZrO_2 berdiri bebas (FSZNTs), campuran oksida tiubnano t-ZrO_2 + a-TiO_2 + amorfus $ZrTiO_2$ dan orthorhombik-$ZrTiO_4$ + a-TiO_2 (ZTNTs), dan campuran oksida tiubnano m-ZrO_2 + α-Fe_2O_3 + Fe_3O_4 (ZFNTs) melalui pengoksidaan anod kerajang-kerajang Zr, Ti-40 wt,% Zr, dan Fe-40 wt.% Zr. Penganodan dilakukan di dalam elektrolit etilena glikol mengandungi F^- pada parameter penganodan yang berbeza i.e. kepekatan NH_4F, jumlah K_2CO_3 atau air, voltan yang dikenakan, dan masa penganodan. Panjang FSZNTs meningkat dari 5.6 ke 12.5 µm dengan peningkatan tempoh penganodan tetapi berkurang dengan peningkatan NH_4F, K_2CO_3, dan voltan yang dikenakan disebabkan pembubaran kimia yang pantas pada antara muka oksida|elektrolit. Manakala, panjang ZTNTs meningkat sehingga 28.6 µm dengan peningkatan tempoh penganodan, voltan yang dikenakan, dan NH_4F tetapi berkurang kepada 7.5 µm dalam 9 vol.% air disebabkan terlebih pembubaran kimia di permukaan ZTNTs. Panjang ZFNTs tidak boleh diukur disebabkan susun atur ZFNTs yang tidak sejajar. Kesan suhu penyepuhlindapan terhadap morfologi, struktur kristal, sifat permukaan, dan sifat optikal tiubnano juga diperiksa dan dikaitkan dengan fotopenurunan Cr(VI). Daripada hasil kajian, amorfus FSZNTs lebih fotoaktif berbanding FSZNTs berhablur di bawah cahaya matahari (95% vs. 30% selepas 5 jam) yang dikaitkan dengan penyerapan Cr(VI) dan penyerapan cahaya yang lebih tinggi. Sebagai tambahan, campuran oksida ZTNTs dan ZFNTs mempamerkan kecekapan penyingkiran Cr(VI) yang lebih tinggi berbanding tiubnano oksida tulen seperti tiubnano ZrO_2 (ZNTs), tiubnano TiO_2 (TNTs), dan tiubnano α-Fe_2O_3 + Fe_3O_4 (FNTs) ditumbuh masing-masing di atas Zr, Ti, dan Fe yang dikaitkan dengan penyerapan Cr(VI) yang lebih baik dan pemisahan pembawa cas yang lebih tinggi. ZTNTs yang disebuhlindap pada 600 °C mempunyai kecekapan penyingkiran Cr(VI) lebih tinggi berbanding ZTNTs yang disepuhlindap pada 400 °C (100% vs. 53% selepas 5 h) bererti kekuatan penyerapan UV oleh fasa orthorhombik-$ZrTiO_4$. Sama juga dengan ZFNTs yang disepuhlindap pada 600 °C mempunyai kecekapan penyingkiran Cr(VI) yang sedikit tinggi berbanding ZFNTs yang disepuhlindap pada 400 °C (86% vs. 83% selepas 3 h) disebabkan kandungan fasa aktif cahaya nampak α-Fe_2O_3 yang lebih tinggi. Berbanding semua sampel, campuran oksida ZFNTs dianggap sebagai foto-pemangkin yang terbaik disebabkan penyerapan Cr(VI) yang sangat baik dan fotoaktiviti yang tinggi di bawah cahaya matahari.

ANODIC ZIRCONIUM DIOXIDE-BASED NANOTUBES FOR PHOTOREDUCTION OF HEXAVALENT CHROMIUM (Cr(VI))

ABSTRACT

Contamination of water by harmful heavy metal ions like hexavalent chromium, Cr(VI) is one of the major global concerns. Exposure to Cr(VI) can cause severe health problems as Cr(VI) is carcinogen. Removal of Cr(VI) from point of wastewater discharged is therefore required. One of the method to remove Cr(VI) from industrial wastewater is by reducing Cr(VI) to less harmful Cr(III) on a suitable photocatalyst. ZrO_2-based nanotubes were fabricated for Cr(VI) photoreduction: freestanding ZrO_2 nanotubes (FSZNTs), mixed oxides t-ZrO_2 + a-TiO_2 + amorphous $ZrTiO_2$ nanotubes and orthorhombic-$ZrTiO_4$ + a-TiO_2 nanotubes (ZTNTs), and mixed oxides m-ZrO_2 + α-Fe_2O_3 + Fe_3O_4 nanotubes (ZFNTs) by anodization of Zr, Ti-40 wt.% Zr, and Fe-40 wt.% Zr foils respectively. Anodization was conducted in F^- containing ethylene glycol electrolyte at varying anodization parameters i.e. NH_4F concentration, K_2CO_3 or water volume, applied voltage, and anodization time. Length of FSZNTs increased from 5.6 to 12.5 µm with increasing anodization time but decreased at high NH_4F, high K_2CO_3, and high applied voltage due to accelerated chemical dissolution at oxide|electrolyte interface. Whereas, the ZTNTs length increased up to 28.6 µm with increasing anodization time, applied voltage, and NH_4F but decreased to 7.5 µm in 9 vol.% water due to excessive chemical dissolution at ZTNTs surface. Length of ZFNTs cannot be measured due to non-aligned ZFNT arrays. The effect of annealing temperature on morphology, crystal structure, surface properties, and optical properties of the nanotubes also were examined and correlated to photoreduction of Cr(VI). From the

results, the amorphous FSZNTs with BET surface area 25.3 m^2/g were more photoactive than the crystalline FSZNTs under sunlight (95% vs. 30% after 5 h) that attributed to enhanced Cr(VI) adsorption and enhanced light absorption. In addition, the mixed oxide ZTNTs and ZFNTs exhibited higher Cr(VI) removal efficiency than pure oxide nanotubes like ZrO_2 nanotubes (ZNTs), TiO_2 nanotubes (TNTs), and α-Fe_2O_3 + Fe_3O_4 nanotubes (FNTs) grown on Zr, Ti, and Fe foils, respectively that ascribed to high Cr(VI) adsorption and enhanced charge carriers separation. ZTNTs annealed at 600 °C has higher Cr(VI) removal efficiency than the ZTNTs annealed at 400 °C (100% vs. 53% after 5 h) implies strong UV absorption of orthorhombic-$ZrTiO_4$ phase. Similarly, the Cr(VI) removal efficiency of ZFNTs annealed at 600 °C slightly higher than ZFNTs annealed at 400 °C (86% vs. 83% after 3 h) due to higher concentration of visible light active α-Fe_2O_3 phase. Among all samples, the mixed oxide ZFNTs were considered as the best photocatalyst due to excellent Cr(VI) adsorption and high photoactivity under sunlight.

CHAPTER ONE

INTRODUCTION

1.1 Research background

In recent years, contamination of surface and ground waters by heavy metal ions like hexavalent chromium, Cr(VI) has attracted the attention from scientists, public, and government agencies as Cr(VI) is toxic and carcinogenic. It can induced many harmful effects to human beings and animals. Cr(VI) ions usually found in poorly treated wastewater released by industries like textile, leather tanning, paint, pigment manufacturing, photography, chrome plating, corrosion protection, wood preservation, fertilizers (Alanis *et al.*, 2013), and metallurgy (Ketir *et al.*, 2012). Since Cr(VI) ions are non-biodegradable, they can be bioaccumulated then biomagnified in animal or plant tissues. This happens when Cr(VI) ions are taken up by human or aquatic animals and stored faster than they are metabolized or excreted.

Cr(VI) has been classified as a Group 1 human carcinogen by the International Agency for Research on Cancer (IARC) and as a Group A inhalation carcinogen by the United State Environmental Protection Agency (US-EPA) (Lakshmanraj *et al.*, 2009). On the other hand, consumption of Cr(VI) can leads to serious health effects such as skin and stomach irritation or ulceration, dermatitis, liver damage, kidney circulation, nerve tissue damage, and death (Owlad *et al.*, 2009).

According to the World Health Organization (WHO) (WHO, 2011) and Malaysian Drinking Water Quality Standard (Division, 2010), the permissible limit of Cr(VI) in drinking water is 0.05 mg/L. However, the concentration of Cr(VI) released by industries usually exceeds the permissible limit due to improper wastewater treatment prior discharge to surface water.

Various methods have been employed to remove Cr(VI) from wastewater including chemical reduction and precipitation, coagulation, membrane separation, oxidation-reduction, ion exchange, electrochemical, and adsorption (Alanis *et al.*, 2013). Nonetheless, some of these methods provide serious sludge generation, exhausted materials disposal, and high operational costs that restricts their actual application (Alanis *et al.*, 2013).

Photoreduction is considered as a clean and efficient method to remove Cr(VI) despite in small concentration. This process requires free electrons for reduction of Cr(VI). This can be achieved by utilize the photogenerated electrons in the conduction band (CB) of a semiconductor (Barakat, 2011). As shown in Figure 1.1, illumination of semiconductor with photon energy greater than the band gap of semiconductor leads to an excitation of electron (e^-) from the valence band (VB) to the CB of a semiconductor producing a hole (h^+) in the VB. The photogenerated electron-hole (e^- - h^+) pairs are then migrated to the semiconductor surface and under suitable redox potential, Cr(VI) is reduced to a less harmful trivalent chromium, Cr(III). Simultaneously, the photogenerated holes will oxidize water into oxygen (Botta *et al.*, 1999).

ZrO_2 is a wide band gap semiconductor (E_g = ~5 - 6 eV) and possesses a highly negative CB edge level that beneficial for reduction (Gionco *et al.*, 2013). As shown in Figure 1.2, the CB edge level for ZrO_2 is -1.0 eV versus (vs.) normal hydrogen electrode (NHE) at pH = 0 which is more negative than TiO_2 and Fe_2O_3. The reduction potential of Cr(VI) to Cr(III) in the form of ions $HCrO_4^-/Cr^{3+}$ under the standard condition is E^0 = +1.35 V vs. NHE at pH = 0 (Vanysek, 2000). For efficient Cr(VI) photoreduction, the CB potential of semiconductor must be more cathodic than the reduction potential of Cr(VI)/Cr(III) (Cheng *et al.*, 2015). Therefore, ZrO_2 has higher reduction potential of Cr(VI) than TiO_2 and Fe_2O_3 despite the band gap of TiO_2 and Fe_2O_3 is much smaller than ZrO_2. This is the main reason of producing ZrO_2-based photocatalysts for remediation of Cr(VI) in wastewater.

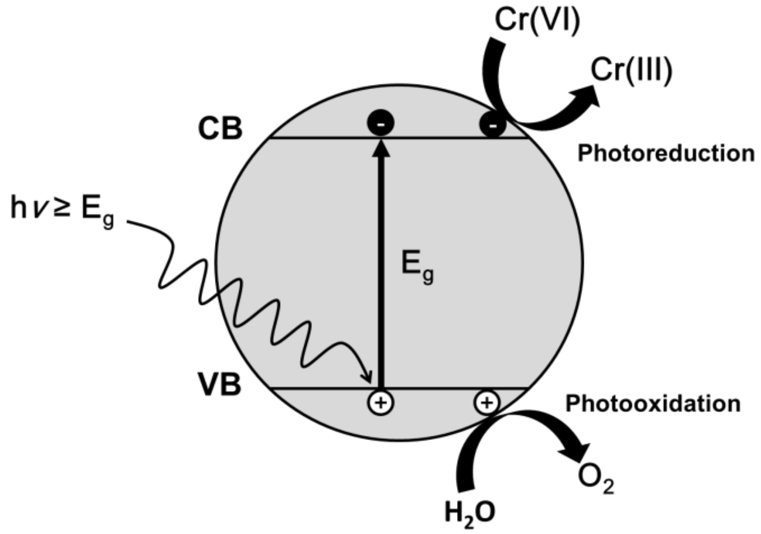

Figure 1.1: Mechanism of Cr(VI) photoreduction under illumination with photon energy greater than the band gap of semiconductor (Shaban, 2013)

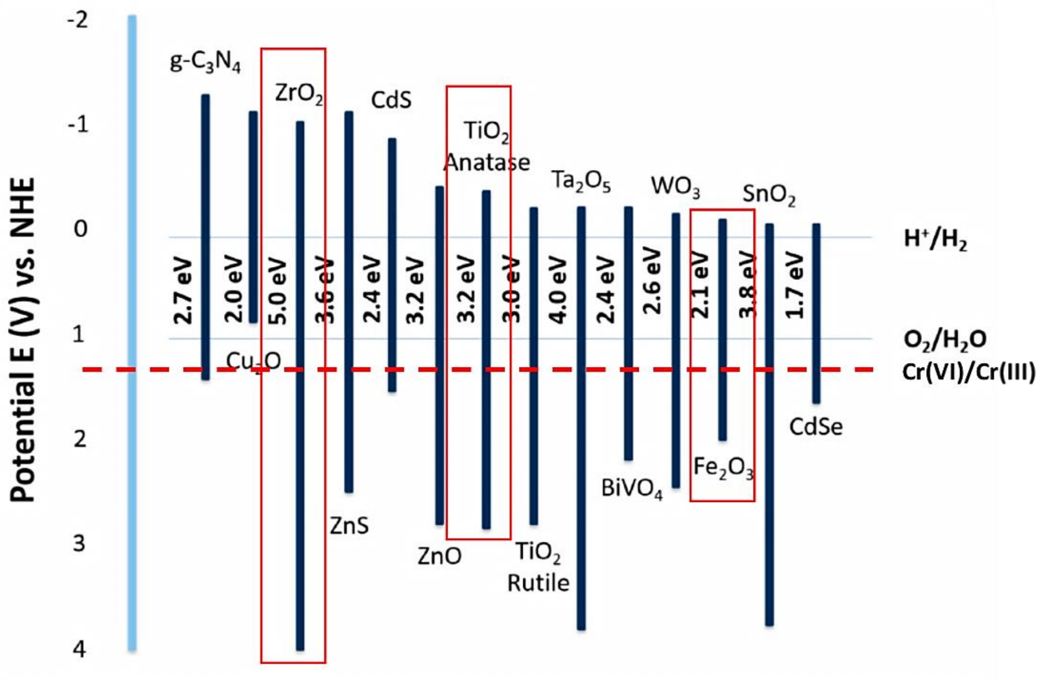

Figure 1.2: CB and VB edges for various semiconductors with respect of reduction potential of Cr(VI) to Cr(III). Adapted from (Jafari *et al.*, 2016)

Fabrication of ZrO_2 photocatalysts in the form of one-dimensional (1-D) nanotubes (NTs) have become a research interest due to their large surface area, unidirectional electron transport, high active sites, and better charge carriers separation (Roy *et al.*, 2010). High surface curvature of NTs contribute to quantum size effects. It generally alters the electronic properties of the semiconductor making them much more reactive to perform redox reaction on their surfaces (Roy *et al.*, 2011).

ZrO_2 nanotubes (ZNTs) can be synthesized by templated (Rao *et al.*, 1997) or anodization (Tsuchiya and Schmuki, 2004) methods. Anodization is a process of growing metal oxide on metal surface in a suitable electrolyte under certain applied voltage. Typical morphologies of anodic NT arrays grown on a metal foil are shown in Figure 1.3 (Fang *et al.*, 2012b). As seen, the anodic oxide film comprised of closed-pack self-organized NT arrays that grown perpendicular on metal substrate. The NTs exhibit an opened-top and closed-bottom in the scallop shaped.

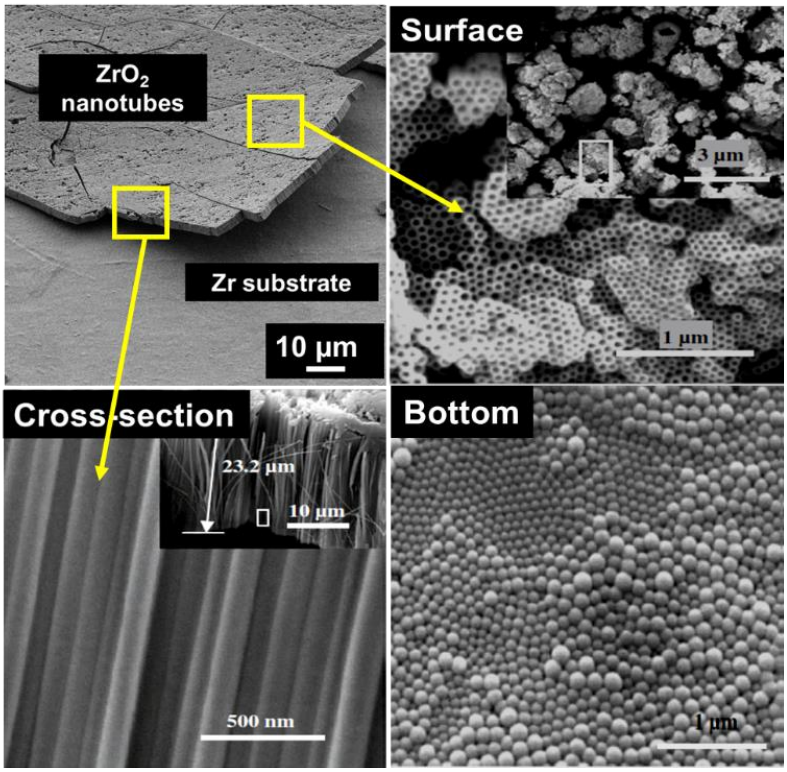

Figure 1.3: Typical morphologies of anodic NTs grown on a metal foil (adapted from Fang *et al.* (2012b)

1.2 Problem statement

Efficiency of photocatalyst usually reduced due to limited visible light harvesting and fast recombination of photoinduced charge carriers. Despite ZrO_2 possesses the highly negative CB edge level than other oxide semiconductors (Figure 1.2), the wide band gap ZrO_2 (E_g = ~5 - 6 eV) (Inagaki *et al.*, 1991;Vempati *et al.*, 2015) restricts its activation under UV light that accounts for less than 5% of solar radiation (Chen *et al.*, 2010). The use of an artificial light source only adds into the complexity of wastewater treatment plant. Thus, sunlight activated photocatalysts are more preferred. To the best of knowledge, there are very limited works on Cr(VI) photoreduction over pure ZrO_2 apart Botta *et al.* (1999) and Karunakaran *et al.* (2009). To date, none work reported on Cr(VI) photoreduction over ZrO_2 nanotubes (ZNTs) under visible light.

Numerous efforts have been devoted to extend the visible light harvesting of ZrO_2 including: (i) coupling with lower band gap oxides (Vignesh *et al.*, 2013) such as ceria (CeO_2) (Wang *et al.*, 2013b;Hao *et al.*, 2017), zinc oxide (ZnO) (Sherly *et al.*, 2014;Ibrahim, 2015), lead dioxide (PbO_2) (Kaviyarasu *et al.*, 2017), bismuth oxide (Bi_2O_3) (Vignesh *et al.*, 2013), and TiO_2 (Zhang *et al.*, 2015;Li *et al.*, 2015;Ji *et al.*, 2017), or (ii) doping with metal (Xiao *et al.*, 2015) or non-metal (Agorku *et al.*, 2015) elements. For these reasons, titanium dioxide (TiO_2) and hematite (α-Fe_2O_3) are the suitable candidates for formation of mixed oxide ZrO_2 photocatalysts due to their lower energy band gaps; 3.2 eV (Wu *et al.*, 2013) and 2.2 eV (Zhang *et al.*, 2010), respectively.

Since discovery of photocatalytic water splitting on TiO_2 electrode in 1972 (Fujishima, 1972), anatase (a)-TiO_2 is the most studied photocatalyst due to its high photoactivity under UV, high stability towards photocorrosion, and low cost

(Hernández-Ramírez and Medina-Ramírez, 2015). Nevertheless, inefficient charge separation and limited range of light absorption are still a major challenge that diminishing the photocatalytic activity of TiO_2. Whereas, due to narrow band gap of α-Fe_2O_3, it can be activated under visible light that collects up ~40% of the total solar energy. It also has high resistivity to corrosion, low toxicity, and perhaps the cheapest semiconductor because of its abundance in environment (Zhang *et al.*, 2010;Xie *et al.*, 2014). However, it suffers poor electron mobility that become the major challenge for its practical application (Zhang *et al.*, 2010). Hence, the combination of ZrO_2 with α-Fe_2O_3 could improve the photocatalytic activity of α-Fe_2O_3.

It is generally accepted the photocatalytic performance of semiconductor is depending on light absorption range, reducibility, and oxidicability of species based on the CB and VB levels of the semiconductor (Li *et al.*, 2017). In order to reduce Cr(VI) to Cr(III), the CB level of semiconductor must be more cathodic than the reduction potential of Cr(VI)/Cr(III) in the form of bichromate ($HCrO_4^-$)/Cr^{3+}) ions which is $E^0 = +1.35$ V vs. NHE at pH = 0 (Vanysek, 2000). As listed in Table 1.1, the calculated CB levels for ZrO_2, a-TiO_2, and α-Fe_2O_3 are more negative than the reduction potential of Cr(VI)/Cr(III). Thus, all oxides can reduce Cr(VI) as consistent with other researchers (Ai *et al.*, 2008;Mekatel *et al.*, 2012;Djellabi and Ghorab, 2014;Cheng *et al.*, 2015). The equations for determine the CB and VB edges of semiconductor are given in the Appendix A.

Besides can increase the visible light absorption, the combination of two different oxide semiconductors also can suppress the e^- - h^+ recombination at semiconductor-semiconductor heterojunction (Kumar *et al.*, 2016). Long-lived e^- - h^+ pairs are obtained if ZrO_2 is coupled with lower band gap semiconductor that has more negative CB edge level. Hence, the CB electrons can be transferred from the lower band gap semiconductor to the wide band gap ZrO_2 for an effective e^- - h^+ separation (Su *et al.*, 2011).

Table 1.1: List of semiconductors with their corresponding band gap, absorption edge, and the calculated CB and VB energy levels with respect to NHE at pH = 0 (Xu and Schoonen, 2000;Kärkkänen, 2014;Polliotto *et al.*, 2017;Tatarchuk *et al.*, 2018)

Semiconductor	**Band gap (eV)**	**Absorption edge (nm)**	**E_{CB} (eV)**	**E_{VB} (eV)**
m-ZrO_2	5.4	230	-1.30	4.12
t-ZrO_2	6.4	194	-1.79	4.61
α-Fe_2O_3	2.2	539	0.28	2.48
a-TiO_2	3.2	413	-0.29	2.91
ortho-$ZrTiO_4$	3.6	345	-0.49	3.19

As shown in Table 1.1, the CB edges for a-TiO_2 and α-Fe_2O_3 are more positive than ZrO_2. Thus, the CB electrons of a-TiO_2 or α-Fe_2O_3 do not have sufficient energy to be transferred into the higher CB level of ZrO_2. But, it can be overcome by an intermediate energy levels in the band gap of ZrO_2 whereby the CB electrons are transferred to the lower defect levels instead of CB level of ZrO_2 (Thejaswini *et al.*, 2017). While, the photogenerated holes are transferred from the more positive VB of ZrO_2 to the more negative VB of the oxides for e^- - h^+ pair separation. Ortho-$ZrTiO_4$ is also listed in the Table 1.1 as this oxide was discovered after annealing the anodized Zr-40Ti alloy.

Defective and disordered oxide semiconductor has also attracted a great attention from the researchers due to its excellent visible light absorption. It is attributed to the presence of oxygen vacancies and defects in non-stoichiometric oxide leading to band gap narrowing (Wang *et al.*, 2012). For instance, Sinhamapatra *et al.* (2016) synthesized a defective black ZrO_2 powders by magnesiothermic reduction in 5% hydrogen/argon from white ZrO_2 powder. Low band gap of black ZrO_2 (E_g = ~1.5

eV) was attributed to high concentration of oxygen vacancies and surface defects leading to enhanced sunlight absorption and excellent photocatalytic hydrogen production than white stoichiometric ZrO_2 powder (Sinhamahapatra *et al.*, 2016). Hence, it can be anticipated the structural disorder in the oxide is not essentially detrimental for photocatalysis but if made properly can produce the sunlight activated oxide semiconductor.

Most of the photocatalytic studies usually performed on crystalline ZrO_2 while little attention has been paid on amorphous ZrO_2. It is commonly accepted the amorphous oxide tend to have low photocatalytic activity due to fast charge carrier's recombination at the defect centers (Ohtani *et al.*, 1997;Ghuman and Singh, 2013). Conversely, enhanced photocatalytic activity of the amorphous oxide was reported on photoreduction of Cr(VI) (Samarghandi *et al.*, 2015), photodegradation of methylene blue (Buddee *et al.*, 2011), and photodegradation of rhodamine B and 4-chlorophenol (Shao *et al.*, 2015) that attributed to increased adsorption sites and efficient Cr(VI) reduction by photogenerated CB electrons (Samarghandi *et al.*, 2015).

Influence of ZrO_2 polymorphs, e.g., tetragonal (t-ZrO_2), monoclinic (m-ZrO_2), and cubic (c-ZrO_2) on photodegradation of methyl orange (MO) under UV light was reported by Basahel *et al.* (2015) and Rozana *et al.* (2017). Nevertheless, there is no general consensus on the most photoactive ZrO_2 polymorphs. According to Basahel *et al.* (2015), m-ZrO_2 was the most photoactive polymorph. Whereas, as oppose to Basahel *et al.* (2015), t-ZrO_2 has higher photocatalytic activity than m-ZrO_2 (Rozana *et al.*, 2017). Therefore, the influence of ZrO_2 polymorphs was investigated towards photoreduction of Cr(VI) by varying the annealing temperature of freestanding ZNTs (FSZNTs).

Despite there are several reports that investigate the effect of anodization parameters (i.e. ammonium fluoride (NH_4F) concentration, water content, applied voltage, and anodization time) on ZNTs formation, no systematic study was made for ZNTs grown in ethylene glycol (EG)/NH_4F added to it potassium carbonate (K_2CO_3) except Soaid *et al.* (2017). The author focused on the effect of K_2CO_3 volume on adhesion and dimension of the ZNTs for photocurrent and photodegradation of MO (Soaid *et al.*, 2017). Similarly, apart from Grigorescu *et al.* (2013), none work reported on the effect of anodization parameters on Ti-Zr alloy grown in F^- containing EG electrolyte. Grigorescu *et al.* (2013) only focused on the influence of applied voltage on diameter of ZTNTs for antibacterial application (Grigorescu *et al.*, 2013). To date, only Guo *et al.* (2013) reported on NTs grown on Fe-Zr alloy in F^- containing EG. But, no systematic studies have been carried out by the authors on the effect of anodization parameters towards morphology of anodized Fe-Zr. As mentioned, this thesis attempted to record all observation on oxide growth on Zr-alloys.

1.3 Research objectives

The objectives of this research are:

i. To synthesis the FSZNTs, mixed oxide ZTNTs, and mixed oxide ZFNTs by anodic oxidation of Zr, Ti-40 wt.% Zr, and Fe-40 wt.% Zr foils in F^- containing EG electrolyte.
ii. To optimize the FSZNTs, mixed oxide ZTNTs, and mixed oxide ZFNTs by varying the anodization parameters (i.e. NH_4F concentration, K_2CO_3 or water content, applied voltage, and anodization time) and annealing temperature.
iii. To apply the fabricated FSZNTs, ZTNTs, and ZFNTs for photoreduction of Cr(VI) under irradiation of sunlight or UV.

1.4 Thesis outline

This thesis can be divided into five main chapters; Chapter 1 introduces the significant of this research and its objectives. Chapter 2 elaborates some theories or underlying mechanisms on NTs formation and photocatalysis. Literature surveys were included in this chapter to find the research gap. The detail procedures on fabrication of NTs and photoreduction test were explained thoroughly in Chapter 3. Chapter 4 gives the detailed explanation regarding the obtained results. The discussion on the results was divided into three main parts; i) fabrication of FSZNTs by anodic oxidation of Zr in EG/NH_4F/K_2CO_3 electrolyte, ii) fabrication of ZTNTs by anodic oxidation of Ti-40 wt.% Zr alloy in EG/NH_4F/H_2O electrolyte, and iii) fabrication of ZFNTs by anodic oxidation of Fe-40 wt.% Zr in EG/NH_4F/H_2O electrolyte. Finally, Chapter 5 concludes all the research outcomes with some recommendations for future works.

CHAPTER TWO
LITERATURE REVIEW

2.1 Introduction

This chapter starts on describing Cr(VI) pollution in Malaysia, reasons and methods to remove them. Then, the growth of anodic ZNTs and mixed oxide NTs is reviewed in details. Photocatalytic reduction of Cr(VI) over ZrO_2-based photocatalysts is also discussed by examining the related literatures.

2.1.1 Heavy metal pollution in Malaysia

Heavy metal can be defined as a metal that has density more than 5 g/cm^3 (Järup, 2003). It naturally exists in the earth crust and found in soils, rocks, sediments, waters, and microorganisms (Mohammed *et al.*, 2011). But, the main source of heavy metal usually arises from anthropogenic activities like mining, industrial, and agriculture. Heavy metal ions have high mobility and hence they can be transported from one medium to another within environment as illustrated in Figure 2.1 (Kobielska *et al.*, 2018). From point of discharged or leaching, they can enter soil, ground or surface water and subsequently bioaccumulated within living organisms causing toxicity and damage. Despite some of heavy metal ions are essential for human biological system, but if the intake of these heavy metal ions exceeds the provisional maximum tolerable daily intake limit, they can cause toxicity. To make it worse, heavy metal ions are non-biodegradable and have an infinite lifetime hence they are persist in the environment.

Contamination of heavy metal ions in Malaysia have been investigated by a few local researchers. Considerable amount of chromium (Cr) was detected in sediments (Sany *et al.*, 2013), soils (Sow *et al.*, 2013;Hossain *et al.*, 2014), dusts (Latif *et al.*, 2013), fishes (Bashir *et al.*, 2013), groundwater (Isa *et al.*, 2013), cooked rice (Omar *et al.*, 2015), human teeth dentine (Asaduzzaman *et al.*, 2017) and in cigarette (Ismail *et al.*, 2017).

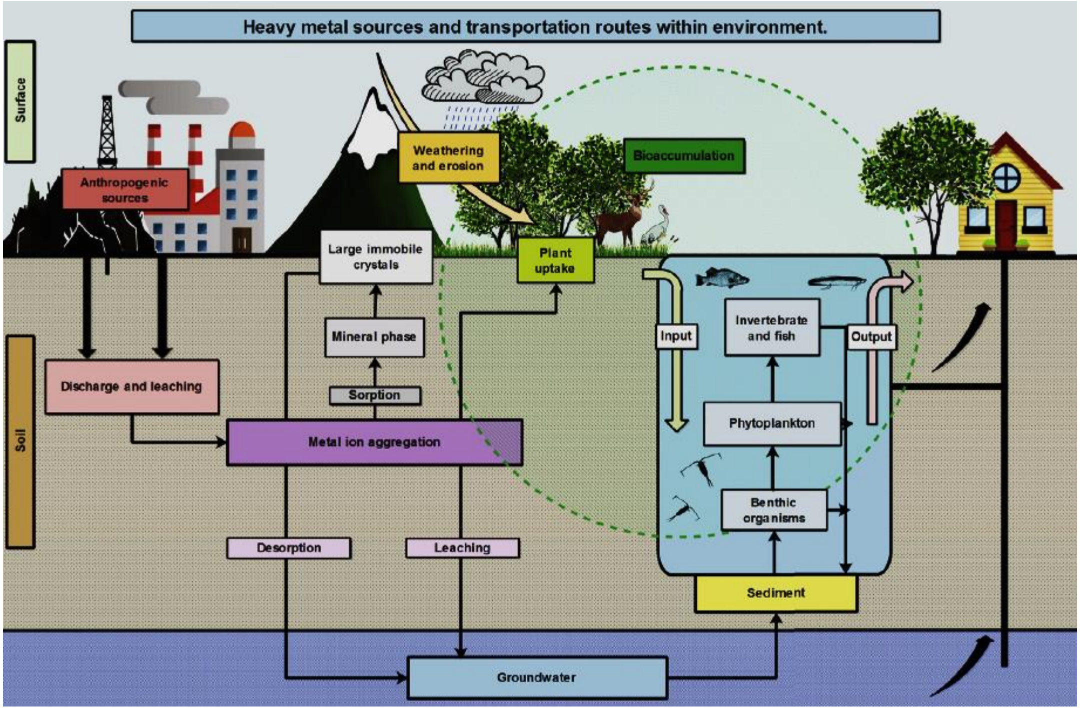

Figure 2.1: Transportation routes for heavy metal ions within environment (Kobielska *et al.*, 2018)

Table 2.1 tabulates the Cr pollution in several states in Malaysia for the past five years (2013 – 2017). As seen, some states heavily contaminated with Cr like Ranau, Sabah (Tashakor *et al.*, 2014), Bukit Rokan and Petasih, Negeri Sembilan (Tashakor *et al.*, 2014), and Rawang, Selangor (Praveena and Aris, 2017) resulting from cocoa plantation, palm oil and rubber plantation, and automotive industry, respectively. The use of pesticides and herbicides to control the insects and weeds in plantation and chrome plating used in automotive industry contribute to Cr(VI) pollution that consequently contaminating river, sediment, and soils. Hence, a proper wastewater treatment must be implemented to curb the Cr(VI) pollution from point of water discharge.

Table 2.1: Cr pollution in several states in Malaysia from year 2013 – 2017

Polluted area	**Cr (mg/kg)**	**Possible sources**	**Ref.**
Port Klang, Selangor	46.4	Industrial wastewater and port activities	(Sany *et al.*, 2013)
Bandar Baru Bangi and Kajang, Selangor	2.0	Electronic and chemical industries	(Latif *et al.*, 2013)
Kuala Lumpur	51.8	Electronic and chemical industries	(Han *et al.*, 2013)
Langat River, Selangor	15.9	Oil palm plantations, shipping, and steelmaking	(Lim *et al.*, 2013)
Gebeng industrial city, Pahang	10.7	Petrochemical plant	(Hossain *et al.*, 2014)
Ranau, Sabah	15145	Cocoa plantation	(Tashakor *et al.*, 2014)
Bukit Rokan and Petasih, Negeri Sembilan	6614	Palm oil and rubber plantation	(Tashakor *et al.*, 2014)
Klang, Selangor	14.0	Electronic and chemical industries	(Yuswir *et al.*, 2015)
Langat River, Selangor	21.0	Oil palm plantations, shipping, and steelmaking	(Kadhum *et al.*, 2015)
Bayan Lepas Free Industrial Zone, Penang	38.0	Electronic and chemical industries	(Khodami *et al.*, 2016)
Kelantan River, Kelantan	63.1	Logging and mining activities	(Wang *et al.*, 2017a)
Rawang, Selangor	501.3	Automotive industry	(Praveena and Aris, 2017)

2.1.2 Hazards of heavy metals

The consumption of animals or plants that have been contaminated by heavy metal ions can cause hazards to human body. The heavy metal ions will be accumulated in human body until reach to toxic level that subsequently induces adverse health deterioration. The continuous exposure to heavy metal ions like As(III), Cd(II), Cr(VI), Pb(II), and Hg(II) can result in several health problems as shown in Table 2.2.

Table 2.2: Toxicities of several heavy metal ions and their permissible limit in water (Division, 2010;WHO, 2011;EPA, 2017)

Heavy metal ion	**Toxicities**	**Permissible limit (mg/L)**		
		US-EPA	**WHO**	**Malaysian Drinking Water Quality Standard**
As(III)	Serious effects of the neurologic, respiratory, hematologic, cardiovascular, and gastrointestinal systems (Gehle, 2009)	0.000	0.01	0.01
Cd(II)	Lung damage, kidney disease, and lung cancer (Registry, 2015b)	0.005	0.003	0.003
Cr(VI)	Skin and stomach irritation or ulceration, dermatitis, liver damage, kidney circulation, nerve tissue damage, and death (Owlad *et al.*, 2009)	0.100	0.05	0.05
Pb(II)	Delays in physical or mental development, children could show slight deficits in attention span and learning abilities, kidney problems, and high blood pressure (Owlad *et al.*, 2009)	0.000	0.01	0.01
Hg(II)	Anxiety, excessive shyness, anorexia, sleeping problems, loss of appetite, irritability, fatigue, forgetfulness, tremors, changes in vision, and changes in hearing (Registry, 2015a)	0.002	0.006	0.001

The continuous exposure to Cr(VI) can leads to skin and stomach irritation or ulceration, dermatitis, liver damage, kidney problem, nerve tissue damage, and death (Owlad *et al.*, 2009). The permissible limit of Cr(VI) in drinking water is 0.05 mg/L as regulated by World Health Organization (WHO) (WHO, 2011) and Malaysian Drinking Water Quality Standard (Division, 2010). Inhaling Cr(VI) on the other hand can induce the formation of cancerous cell as Cr(VI) ions have been classified as a Group 1 human carcinogen by the International Agency for Research on Cancer and as a Group A inhalation carcinogen by the United State Environmental Protection Agency (US-EPA) (Lakshmanraj *et al.*, 2009).

Cr usually exists in the form of Cr(VI) and Cr(III). Cr(VI) is 1000 times more toxic and highly mobile than Cr(III) (Katz and Salem, 1993). As mentioned, Cr(VI) ions in wastewater usually released by industries like steelmaking (Bankole *et al.*, 2014), tanneries, electroplating, leathering, and textile (Ismail *et al.*, 2013). Cr(III) on the other hand naturally occurred in the environment and is one of the essential nutrients for human body (Owlad *et al.*, 2009). Converting Cr(VI) to Cr(III) may pose a solution towards excess of Cr(VI) in the environment. Cr(III) can then be easily removed by precipitation of chromium hydroxide, $Cr(OH)_3$ at high pH (Barrera-Díaz *et al.*, 2012).

2.2 Techniques to remove Cr(VI)

Several methods can be used to remove Cr(VI) from wastewater including adsorption, membrane filtration, ion exchange, electrochemical treatment, and reduction (Owlad *et al.*, 2009). The explanation regarding each method is elaborated as follows.

2.2.1 Adsorption

Adsorption is a process whereby the Cr(VI) ions are concentrated on adsorbent surface (Owlad *et al.*, 2009). Cr(VI) is transferred from bulk solution to an adsorbent solid surface via physical and/or chemical bonding (Barakat, 2011). Several low-cost adsorbents were used to remove Cr(VI) from contaminated wastewater including an agricultural waste, industrial by-product, natural material, or modified biopolymers (Barakat, 2011). The examples of natural adsorbents are clays (Zhao *et al.*, 2013), eggshell membrane (Daraei *et al.*, 2014), rice straw (Elmolla *et al.*, 2016), and Hibiscus Cannabinus kenaf (Omidvar Borna *et al.*, 2016). The examples of industrial by-product adsorbents are dolochar (Panda *et al.*, 2017), cork waste (Sfaksi *et al.*, 2014), and sugar wastes (Anastopoulos *et al.*, 2017). Despite this method is efficient to treat high concentration of Cr(VI) up to 500 ppm (Srivastava *et al.*, 2017), the adsorbent surface still enriched with toxic Cr(VI) that requires further treatment method before discard them to the environment.

2.2.2 Membrane filtration

Membrane filtration is used to remove the suspended solid and inorganic contaminants like heavy metals from wastewater. The removal efficiency is dependent on membrane pore size and molecular weight of the suspended solid. To allow the water passage and filtration of unwanted contaminants, the size of solid contaminants must be larger than the membrane pore size (Barakat, 2011). Several kinds of membranes can be utilized including ultrafiltration (UF), reverse osmosis (RO), and nanofiltration (NF) (Barakat, 2011).

UF is a membrane technique that working at low transmembrane pressure. The heavy metal ions can be passed easily through the UF membranes due to its small size. Whereas, RO uses a semi-permeable membrane that allows the purified water to pass through the membrane while rejecting the contaminants. NF is an intermediate process of UF and RO (Fu and Wang, 2011). This method is suitable for remediation of low Cr(VI) concentration as low as 1 ppm (Li *et al.*, 2016) but suffered to membrane fouling (Fu and Wang, 2011).

2.2.3 Ion exchange

Ion exchange works by exchanging cations between cations exchangers (e.g. synthetic resins, natural zeolites, or montmorillonites) with heavy metal ions in the solution. For synthetic resins, the most common cation exchangers are strongly acidic resins (sulfonic acid groups, i.e., $-SO_3H$) and weakly acid resins (carboxylic acid groups, i.e., -COOH). Hydrogen ions in the functional groups exchange ions with metal cations in the heavy metals (Fu and Wang, 2011). It can efficiently remove Cr(VI) but the ion exchange resins must be reproduced by chemical reagents every time they are exhausted and this will induce serious secondary pollution. Besides, it is also expensive which is not suitable for large scale operation (Fu and Wang, 2011).

2.2.4 Electrochemical treatment

This process can be divided into three established methods (Fu and Wang, 2011):

i. Electrocoagulation (EC) – by generation of coagulants via in-situ. The metal is firstly oxidized to produce the metal ions at anode, and the hydrogen gas is released at cathode. The hydrogen gas is used to float the flocculated particles/precipitates out from water. For instance, Cr(VI) is firstly reduced to Cr(III) at the cathode before precipitated into $Cr(OH_3)$ and removed from the solution by floatation of $Cr(OH_3)$ precipitates.

ii. Electroflotation (EF) – is a solid-liquid separation process, whereby the tiny bubbles of hydrogen and oxygen gases released from water electrolysis are used to float the solid $Cr(OH)_3$ to the water surface.

iii. Electrodeposition (ED) – for solid metal recovery from wastewater. The solid metal is deposited on the cathode surface.

The rapid and high removal efficiency was obtained by using coupled techniques of EC-EF (Aoudj *et al.*, 2015). But, it is not practical for actual application due to its expensive electrical supply.

2.2.5 Reduction

Cr(VI) is a diprotic acid with pK_a value of 5.9. At pH > 6, the main species is tetrahedral ion (CrO_4^{2-}) which causes a yellowish color to the solution. At pH range 6 > pH > 2, bichromate ($HCrO_4^-$) and dichromate ($Cr_2O_7^{2-}$) ions coexist. At pH < 1, the main solute is chromic acid (H_2CrO_4) (Ottonello, 2002). Cr(VI) ions are highly mobile and strong oxidants. Because of this, sorption is rather difficult, making removal via adsorption to be less efficient. On the other hand, Cr(III) forms sparingly soluble solids like $Cr(OH)_3$ which is less mobile. Therefore, redox transformation of Cr(VI) to Cr(III) has been seen as an effective process for controlling the transport of Cr(VI) in the environment. A number of mechanisms have been proposed for reduction of Cr(VI) involving combinations of one, two and three-electrons reduction processes. There is a possibility of one-electron reducing steps from Cr(VI) to Cr(V) then to Cr(IV) and finally to Cr(III) as the stable final product or a single, three-electrons reduction process (Botta *et al.*, 1999). For reduction to happens, electrons must be transferred from a reductant to Cr(VI) ions.

Cr(VI) can be reduced by several well-known reductants that can donate electrons to Cr(VI) compounds. Fe(II) salts or Fe(II) containing solids typically used as reducing materials (Eary and Rai, 1988) and have been successful in the removal of Cr(VI) by chemical reduction process. Nevertheless, the process often leads to significant amount of sludge. Reduction can also occur by humic, organic compounds such as alkanes, alcohols, aldehydes, ketones, and aliphatic and aromatic acids. Reduction by common inorganic acids can also happen.

Apart from chemical reductants, some bacteria have also shown Cr(VI)-reducing activities for examples *escherichia coli* and *agrobacterium radiobacter* (Chirwa and Molokwane, 2011). Although chromium-reducing bacteria are possible to be cultured and applied for Cr(VI) reduction in wastewater, significant amount of bacteria cells are required for an effective treatment. Apart from microbial reduction, plants have also been used to reduce Cr(VI) (Lytle *et al.*, 1998). Reduction of Cr(VI) can also be mediated biologically by various enzymes and nonenzymatic agents derived from plants.

Photocatalytic reduction on the other hand, as introduced, is an alternative route in achieving redox transformation of Cr(VI) to Cr(III). Referring to International Union of Pure and Applied Chemistry (IUPAC), the definition of photocatalysis is the change in the rate of a chemical reaction or its initiation under the action of ultraviolet, visible, or infrared radiation in the presence of a substance - the photocatalyst - that absorbs light and is involved in the chemical transformation of the reaction partners (IUPAC, 1997). This translates to redox reactions that can occur on a surface of a catalyst when it is illuminated with light.

When a semiconductor photocatalyst is illuminated with photon energy greater than the band gap of semiconductor ($h\nu > E_g$), e^- - h^+ pairs will be produced in the CB and VB of semiconductor, respectively (Equation 2.1) (Barakat, 2011). These charge carriers then migrated to the semiconductor surface for redox reaction. Reduction occurs when electrons are transferred to an adsorbed Cr(VI) (Equation 2.2) (Wu *et al.*, 2013), while oxidation occurs when holes are transferred to water (Equation 2.3) (Botta *et al.*, 1999):

$$\text{Semiconductor} \rightarrow e^-_{(CB)} + h^+_{(VB)} \qquad \text{Equation 2.1}$$

$$HCrO_4^- + 7H^+ + 3e^- \rightarrow Cr^{3+} + 4H_2O \qquad \text{Equation 2.2}$$

$$2H_2O + 4h^+ \rightarrow O_2 + 4H^+ \qquad \text{Equation 2.3}$$

In summary, reduction of Cr(VI) in wastewater can therefore be accomplished by:

i. Abiotic reduction (without the presence of life organisms) i.e. by reactions with aqueous ions (Fe^o for example), reduction with organic (humic) substances or electron transfer at semiconductor photocatalysts surfaces or
ii. Biotic reduction (in the presence of life organism) by microbes, enzymes or by plant tissue.

Therefore, the photoreduction process is considered as the most ideal method for Cr(VI) remediation in wastewater as the carcinogenic Cr(VI) can be converted to less harmful Cr(III) without generation of secondary pollutant. The process can be performed under solar irradiation over semiconductor photocatalyst as will be explained in the next section. The advantages and disadvantages of each method are listed in Table 2.3.

Table 2.3: Advantages and disadvantages of heavy metal removal methods (Barakat, 2011;Fu and Wang, 2011)

Method	Advantages	Disadvantages
Adsorption	Low-cost, easy operating conditions, wide pH range, and high metal binding capacities.	Low selectivity and high production of solid wastes.
Membrane filtration	Small space requirement, low pressure, high separation, and high selectivity.	High operational cost due to membrane fouling.
Ion exchange	High treatment capacity, high removal efficiency, and fast kinetics.	Expensive and induce serious secondary pollution.
Electrochemical	Solid metal recovery.	Expensive electrical supply.
Photoreduction	Cr(VI) can be reduced to less toxic Cr(III) with no harmful by products.	Long duration time and limited applications.

2.3 Fundamental of photocatalysis

Photoreduction or photocatalytic reduction involves the process of chemical reduction of Cr(VI) that takes place in the presence of light. Fundamental of photocatalysis is reviewed here in order to explain on how a semiconductor photocatalyst is used to reduce Cr(VI) to Cr(III) under illumination. Illumination of semiconductor photocatalyst with photon energy greater than the band gap of semiconductor brings to excitation of electron in the VB to the CB of semiconductor producing an e^- - h^+ pair. These photogenerated e^- - h^+ pair follows several pathways as illustrated in Figure 2.2 (Linsebigler *et al.*, 1995):

i. “C” is a path where e^- diffuses to semiconductor surface and transfers to an adsorbed acceptor molecule or ion (Acc) (Equation 2.4). This is a process occurs during the Cr(VI) reduction.

ii. "D" is a path where h^+ diffuses to semiconductor surface and accept e^- donated from a donor molecule or ion (Don) (Equation 2.5). Water is oxidized via this process.

$Acc_{(ads)} + e^- \rightarrow Acc^-_{(ads)}$ Equation 2.4

$Don_{(ads)} + h^+ \rightarrow Don^+_{(ads)}$ Equation 2.5

iii. "A' is a path where e^- loses its energy and recombines with h^+ in the VB on photocatalyst surface. This results in annihilation of free carriers. Recombination happens at surface defects such as Zr^{3+} (Gionco *et al.*, 2013).

iv. "B" is also a recombination process but occurs in the bulk of semiconductor. This also results in annihilation of free carriers. Example of bulk defect is oxygen vacancies (Setvín *et al.*, 2017).

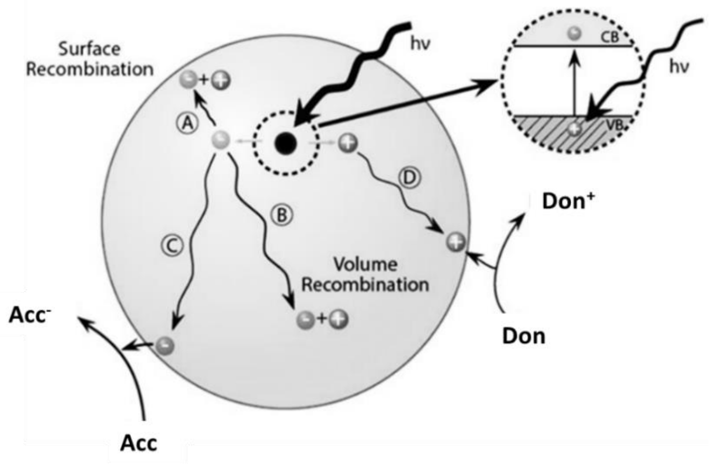

Figure 2.2: Phenomena takes place in a semiconductor photocatalyst. The photogenerated carriers can recombine at a surface trap (A) or in the bulk (B); otherwise, they can interact with acceptor (Acc) or donor (Don) species (Linsebigler *et al.*, 1995)

Annihilation of free carriers is shown (Equation 2.6), where N is the neutral center and E is the energy released in the form of light or heat (Herrmann, 1999). Paths

A and B are therefore unwanted and must be minimized to allow for more e^- and h^+ transfer to photocatalyst surface for chemical processes. Several techniques are developed to suppress the charge carriers' recombination such as producing highly pure semiconductors which is not possible for nanoscale semiconductor, deposition of a noble metal on semiconductor surface, coupling with other oxide, dye sensitization, or doping with metal or non-metal elements (Linsebigler *et al.*, 1995).

$$e^- + h^+ \rightarrow N + E \qquad \text{Equation 2.6}$$

2.3.1 Charge carrier trapping or recombination

As seen in Equation 2.6, recombination of photoinduced charge carriers release energy when electron transit back to the VB. The energy released can be in form of light (radiative recombination) or heat (non-radiative recombination). In a photocatalyst, recombination occurs either at the surface (path A) or bulk (path B). The surface and bulk states are created due to various crystal defects or impurities in the semiconductor (Kasap, 2006). The nanosized materials usually have high structural imperfections and defects derived from sample preparation method (Gionco *et al.*, 2013). Nevertheless, these defects states can also serve as charge carrier traps. Traps can function as a "temporary level" in which electron can reside before jumping back to the VB. Traps can suppress the e^- - h^+ recombination (Linsebigler *et al.*, 1995). The charge carriers can be trapped at shallow or deep/bulk states distributed in the energy gap (or forbidden gap), in which the shallow states are located nearer to band edges (Figure 2.3). This is regarded similar to wide band gap ZrO_2 (Gionco *et al.*, 2017).

As shown in Figure 2.4 , the shallow and bulk states can either act as recombination or trapped centers depending on particular events, either *"a", "b", "c", or "d"* (Kasap, 2006). Kasap (2006) suggested the electron can be trapped and detrapped several times before it finally recombines with a hole in the VB, associated with photon emission.

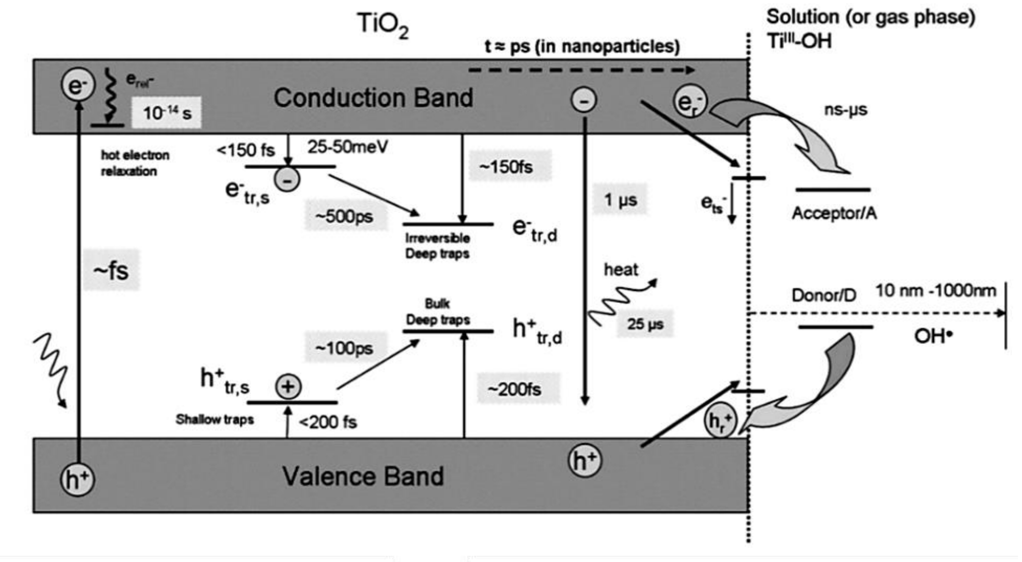

Figure 2.3: Typical time scales for photocatalytic reactions on TiO$_2$ (Paramasivam *et al.*, 2012)

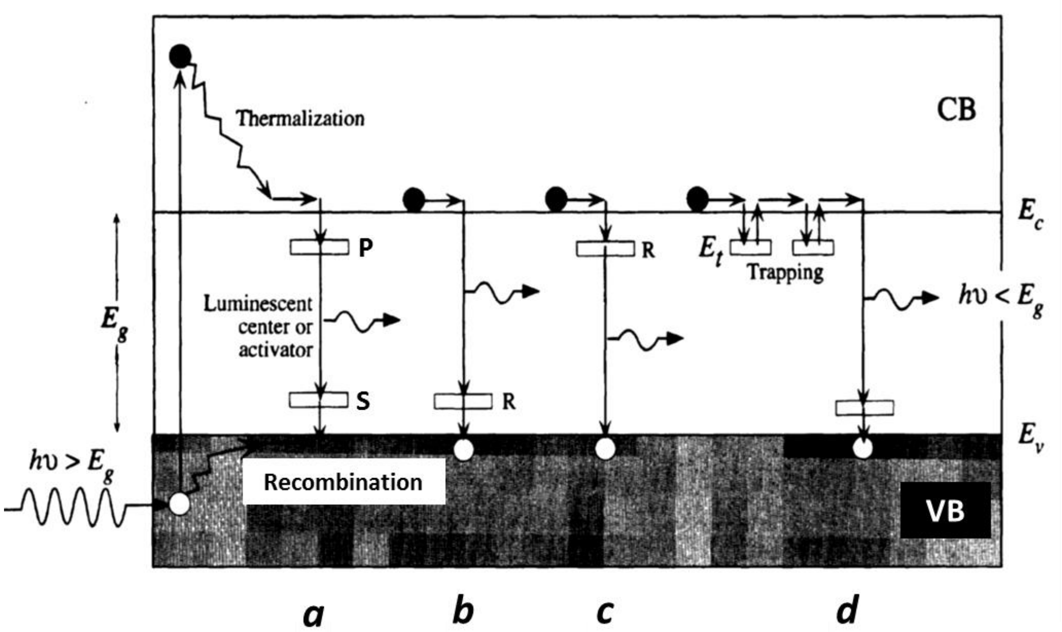

Figure 2.4: Trap and recombination centers in band gap of semiconductor (Kasap, 2006)